



Observation of sizeable ω contribution to $\chi_{c1}(3872) \rightarrow \pi^+ \pi^- J/\psi$ decays

LHCb collaboration[†]

Abstract

Resonant structures in the dipion mass spectrum from $\chi_{c1}(3872) \rightarrow \pi^+ \pi^- J/\psi$ decays, produced via $B^+ \rightarrow K^+ \chi_{c1}(3872)$ decays, are analyzed using proton-proton collision data collected by the LHCb experiment, corresponding to an integrated luminosity of 9 fb^{-1} . A sizeable contribution from the isospin conserving $\chi_{c1}(3872) \rightarrow \omega J/\psi$ decay is established for the first time, $(21.4 \pm 2.3 \pm 2.0)\%$, with a significance of more than 7.1σ . The amplitude of isospin violating decay, $\chi_{c1}(3872) \rightarrow \rho^0 J/\psi$, relative to isospin conserving decay, $\chi_{c1}(3872) \rightarrow \omega J/\psi$, is properly determined, and it is a factor of six larger than expected for a pure charmonium state.

Published in Phys. Rev. D 131 (2023) L011103

© 2023 CERN for the benefit of the LHCb collaboration. CC BY 4.0 licence.

[†]Authors are listed at the end of this paper.

After the discovery of the $\chi_{c1}(3872)$ state in decays through the $\pi^+\pi^-J/\psi$ channel [1], the ρ^0J/ψ process was suggested to explain the observed $\pi^+\pi^-$ mass ($m_{\pi^+\pi^-}$) distribution peaking near the upper kinematic limit, close to the ρ^0 pole mass. The isovector nature of the produced $\pi^+\pi^-$ pairs is also supported by the non-observation of $\chi_{c1}(3872) \rightarrow \pi^0\pi^0J/\psi$ decays. Since no charged partners of the $\chi_{c1}(3872)$ state have been observed in the $\rho^\pm J/\psi$ decay mode [2,3], the $\chi_{c1}(3872)$ particle is predominantly an isosinglet state; the J/ψ isospin is also zero. Together, this makes the $\chi_{c1}(3872) \rightarrow \rho^0J/\psi$ decay isospin violating. The $\chi_{c1}(3872)$ spin and parities, $J^{PC} = 1^{++}$ [4,5], match the 2^3P_1 excitation of the $c\bar{c}$ system predicted in the relevant mass range [6]. However, isospin violating decays of charmonium states are highly suppressed. Therefore, quantifying the isospin violation in $\chi_{c1}(3872) \rightarrow \rho^0J/\psi$ decays is important to understand the nature of the $\chi_{c1}(3872)$ state, which is under intense debate [7,8]. Isospin conserving $\chi_{c1}(3872) \rightarrow \omega J/\psi$ decays provide a suitable normalization process. Such decays have been recently established with a significance of 5σ [9] using the dominant $\omega \rightarrow \pi^+\pi^-\pi^0$ decay, which has a branching fraction (\mathcal{B}) of $(89.2 \pm 0.7)\%$ [10]. Averaged with earlier measurements [11,12], $\mathcal{B}(\chi_{c1}(3872) \rightarrow \omega J/\psi)/\mathcal{B}(\chi_{c1}(3872) \rightarrow \pi^+\pi^-J/\psi) = 1.4 \pm 0.3$. However, $\omega \rightarrow \pi^+\pi^-$ decays, with $\mathcal{B}(\omega \rightarrow \pi^+\pi^-) = (1.53 \pm 0.12)\%$ [10], are expected to contribute to the denominator at the 2% level if $\rho^0 - \omega$ interference is neglected. The interference can change this estimate by a large factor. Therefore, an analysis of the $m_{\pi^+\pi^-}$ spectrum is necessary to disentangle the ρ^0 and ω contributions. Such analyses were performed by the CDF [13] and the Belle [3] collaborations, using the Breit–Wigner sum model, yielding inconclusive results due to the large statistical uncertainties.

In this Letter, we report an analysis of a $B^+ \rightarrow K^+\chi_{c1}(3872)$, $\chi_{c1}(3872) \rightarrow \pi^+\pi^-J/\psi$, $J/\psi \rightarrow \mu^+\mu^-$ data sample collected using the LHCb detector, with proton-proton (pp) collision energies of 7, 8 and 13 TeV, corresponding to a total integrated luminosity of 9 fb^{-1} . The inclusion of charge-conjugate processes is implied throughout. This sample is about six times more sensitive to an ω contribution than those used in Refs. [3,13]. The LHCb detector [14,15] is a single-arm forward spectrometer covering the pseudorapidity range $2 < \eta < 5$, designed for the study of particles containing b or c quarks. The detector elements that are particularly relevant to this analysis are: a silicon-strip vertex detector surrounding the pp interaction region that allows b hadrons to be identified from their characteristically long flight distance; a tracking system that provides a measurement of the momentum, p , of charged particles; two ring-imaging Cherenkov detectors that are able to discriminate between different species of charged hadrons and the muon detector.

The selection of $\chi_{c1}(3872) \rightarrow \pi^+\pi^-J/\psi$ candidates is based on the reconstruction of $B^+ \rightarrow K^+\pi^+\pi^-J/\psi (\rightarrow \mu^+\mu^-)$ decays, which provides for efficient background suppression and optimal dipion mass resolution. Both muon candidates are identified by the muon detector. The dimuon mass must be consistent with the known J/ψ mass [10], and all five final state particles must form a good-quality vertex significantly displaced from the closest primary pp interaction vertex (PV). The hadron candidate most likely to be a kaon is selected as the kaon candidate. Each hadron must have a significant impact parameter with respect to any PV. To remove multiple entries per event, the B^+ candidate with the largest scalar sum of the hadron and J/ψ candidate transverse-momenta is selected. To improve mass resolution, the B^+ candidates are kinematically constrained to point to the closest PV and reproduce the known J/ψ mass [16]. The mass of these candidates must be consistent with the known B^+ mass [10], which is then also included among the kinematic constraints. The resulting $m_{\pi^+\pi^-J/\psi}$ distribution (Fig. 1) is fit with a signal

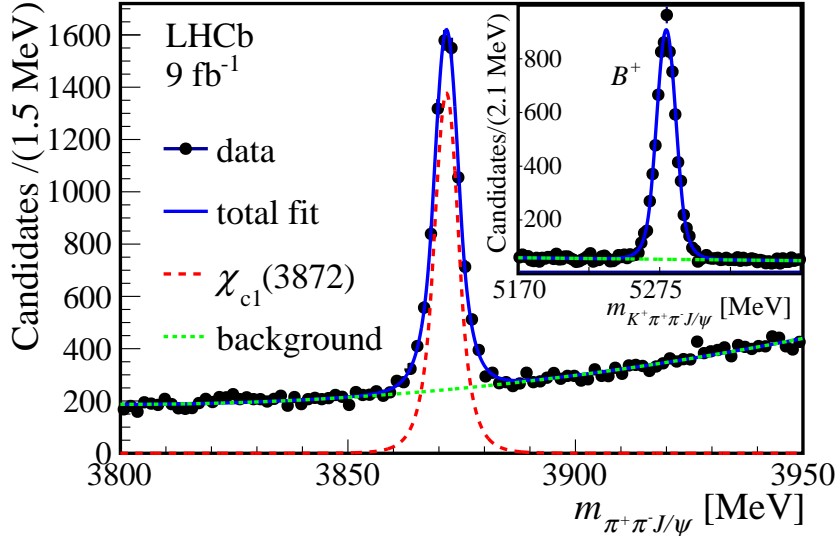


Figure 1: Distribution of $m_{\pi^+\pi^- J/\psi}$ ($m_{K^+\pi^+\pi^- J/\psi}$ in the inset) from $B^+ \rightarrow K^+\pi^+\pi^- J/\psi$ candidates within $\pm 2\sigma$ around the B^+ ($\chi_{c1}(3872)$) mass, overlaid with the fit including the total (solid blue), signal (dashed red) and background (dashed green) components.

(background) shape modelled by a double-sided Crystal Ball [17] (quadratic) function, yielding 6788 ± 117 $\chi_{c1}(3872) \rightarrow \pi^+\pi^- J/\psi$ decays with a $\chi_{c1}(3872)$ mass resolution of $\sigma_m = 2.66 \pm 0.09$ MeV (natural units are used throughout). The signal purity is 77% within $\pm 2\sigma_m$ around the $\chi_{c1}(3872)$ mass. The dominant source of background is from B^+ decays to J/ψ meson and excited kaons (K^{*+}), which decay to $K^+\pi^+\pi^-$. The dipion mass distribution is obtained by two-dimensional unbinned fits of the $\chi_{c1}(3872)$ signal yields to the $(m_{\pi^+\pi^- J/\psi}, m_{\pi^+\pi^-})$ data in $m_{\pi^+\pi^-}$ intervals. The signal shape in $m_{\pi^+\pi^- J/\psi}$ is fixed to the global fit result of Fig. 1, while the background shape may vary in each $m_{\pi^+\pi^-}$ interval. The signal and the background $m_{\pi^+\pi^- J/\psi}$ shapes are then multiplied by a two-body phase-space factor, *i.e.* the J/ψ momentum in the $\chi_{c1}(3872)$ rest frame ($p_{J/\psi}$), which depends on both $m_{\pi^+\pi^- J/\psi}$ and $m_{\pi^+\pi^-}$. The resultant shapes are normalized to unity using their integral over the fitted phase-space range. The obtained data points are shown in Fig. 2.

Signal simulation is used to obtain the $m_{\pi^+\pi^-}$ dependence of the dipion mass resolution and of the reconstruction efficiency. In the simulation, pp collisions are generated using PYTHIA [18] with a specific LHCb configuration [19]. Decays of unstable particles are described by EVTGEN [20], in which final-state radiation is generated using PHOTOS [21]. In particular, $B^+ \rightarrow K^+\chi_{c1}(3872)$, $\chi_{c1}(3872) \rightarrow J/\psi\rho^0$, $\rho^0 \rightarrow \pi^+\pi^-$, $J/\psi \rightarrow \mu^+\mu^-$ signal decays are simulated using the helicity model where the $\chi_{c1}(3872)$ decays via an S -wave, which describes the angular distributions in the data well [5]. When integrating over $m_{\pi^+\pi^-}$, the generated $m_{\pi^+\pi^-}$ distribution is weighted to reproduce the observed distribution. The interaction of the generated particles with the detector, and its response, are implemented using the GEANT4 toolkit [22] as described in Ref. [23]. The underlying pp interaction is reused multiple times, with an independently generated signal decay for each event [24]. The transverse-momentum distribution of the signal B^+ is weighted to match the data. The relative signal reconstruction efficiency obtained from the simulation is well described by a quadratic function,

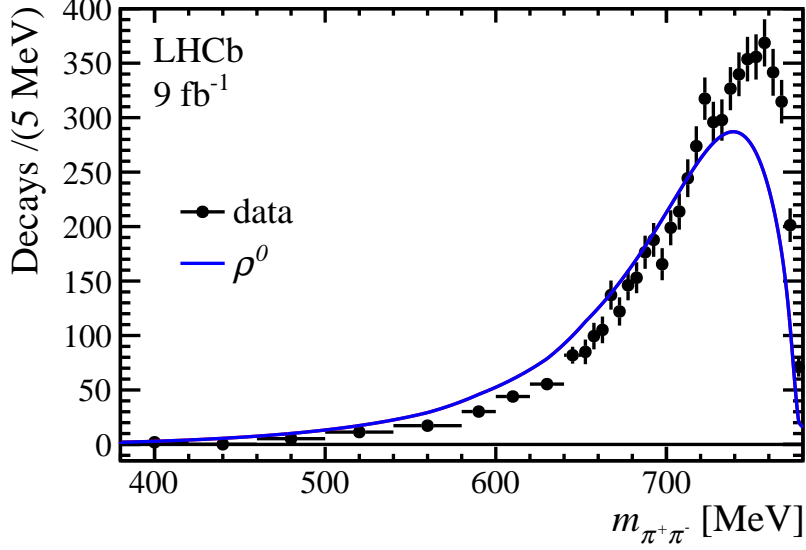


Figure 2: Distribution of $m_{\pi^+\pi^-}$ in $\chi_{c1}(3872) \rightarrow \pi^+\pi^- J/\psi$ decays, fit with the ρ^0 -only model.

$\epsilon(m_{\pi^+\pi^-}) = 0.966 + 1.345 \times 10^{-3} (m_{\pi^+\pi^-} - 700) + 1.607 \times 10^{-6} (m_{\pi^+\pi^-} - 700)^2$, and the dipion mass resolution by $\sigma(m_{\pi^+\pi^-}) = 2.39 (1 - \exp(-m_{\pi^+\pi^-}/220.3)) - 5.4 \exp(-m_{\pi^+\pi^-}/220.3)$, where $m_{\pi^+\pi^-}$ and $\sigma(m_{\pi^+\pi^-})$ are in MeV. The simulation underestimates the $\chi_{c1}(3872)$ and B^+ mass resolution by 6% and 14%, respectively. Therefore, $\sigma(m_{\pi^+\pi^-})$ is scaled up by $f_m = 1.06$, which is varied from 1.00 to 1.14 to assess a systematic uncertainty. All theoretical probability density functions fit to the data, $\mathcal{P}(m_{\pi^+\pi^-})$, are multiplied by the relative efficiency function, $\epsilon(m_{\pi^+\pi^-})$ and convolved with a Gaussian distribution characterized by a root-mean-square value of $f_m \sigma(m_{\pi^+\pi^-})$.

The matrix element, \mathcal{M} , describing the three-body decay, $\chi_{c1}(3872) \rightarrow \pi^+\pi^- J/\psi$, is related to $\mathcal{P}(m_{\pi^+\pi^-})$ via a scaling (S) and the phase-space factors, $\mathcal{P}(m_{\pi^+\pi^-}) = S p_{J/\psi} p_\pi |\mathcal{M}|^2$, where p_π is the pion momentum in the rest frame of the $\pi^+\pi^-$ system. The scaling factor S is a nuisance parameter.

Following the previous analyses [3, 13], the ρ^0 component is first parameterized as a Breit–Wigner (BW) amplitude,

$$\mathcal{M} = \text{BW}(s | m_\rho, \Gamma_\rho) = \frac{m_\rho \Gamma_\rho \sqrt{B_1(p_\pi)/B_1(p_\pi^\rho)}}{m_\rho^2 - s - i m_\rho \Gamma(s)}, \quad \Gamma(s) = \Gamma_\rho \frac{p_\pi}{p_\pi^\rho} \frac{m_\rho}{\sqrt{s}} \frac{B_1(p_\pi)}{B_1(p_\pi^\rho)}, \quad (1)$$

where $s \equiv m_{\pi^+\pi^-}^2$, $p_\pi^\rho = p_\pi(m_\rho)$, $m_\rho = 775.26$ MeV, $\Gamma_\rho = 147.4$ MeV [10] and $B_1(p) = p^2 / [1 + (Rp)^2]$ is the Blatt–Weisskopf barrier factor for the P -wave decay of a vector particle to $\pi^+\pi^-$, and contains an effective hadron-size parameter R . With R adjusted to 1.45 GeV $^{-1}$, a complex phase of the BW amplitude varies in the fitted $m_{\pi^+\pi^-}$ range within one degree of the isovector $\pi^+\pi^-$ P -wave parametrization extracted from the scattering data by the phenomenological analysis of Ref. [25]. A similar value of 1.5 GeV $^{-1}$ was used in the previous analyses [3, 13]. The χ^2 fit, with S as the only fit parameter, fails to describe the data as shown in Fig. 2, with a χ^2 value per number of degrees of freedom (χ^2/NDoF) equal to $366.6/34$. A large disagreement between the data and the $\chi_{c1}(3872) \rightarrow \rho^0 J/\psi$ amplitude at high dipion masses was missed in the previous comparisons with the $\chi_{c1}(3872) \rightarrow \rho^0 J/\psi$ simulation (see Fig. S2 in the supplementary

material of Ref. [5]; see also Refs. [26, 27]), because the EVTGEN [20] model does not correctly simulate the impact of the phase-space factors (here $p_{J/\psi} p_\pi$) on resonant shapes. As a consequence, the large $\rho^0 - \omega$ interference in the data (see below) was mistakenly interpreted as a part of the ρ^0 resonance itself.

Adding an ω contribution via the BW sum model with $\mathcal{M} = \text{BW}(s|m_\rho, \Gamma_\rho) + a \exp(i\phi) \text{BW}(s|m_\omega, \Gamma_\omega)$, where a and ϕ are the amplitude and phase of the ω component relative to the ρ^0 term [3, 13], improves the fit quality substantially, $\chi^2/\text{NDoF} = 102.9/33$, yet not enough to be acceptable. Summing BW amplitudes results in matrix elements that are not unitary, violating first principles of scattering theory. A two-channel K -matrix (K) model [28], coupling the $\pi^+\pi^-$ and $\pi^+\pi^-\pi^0$ channels via an ω contribution, resolves this issue,

$$K = \frac{1}{m_\rho^2 - s} \begin{pmatrix} g_{\rho \rightarrow 2\pi}^2 & 0 \\ 0 & 0 \end{pmatrix} + \frac{1}{m_\omega^2 - s} \begin{pmatrix} g_{\omega \rightarrow 2\pi}^2 & g_{\omega \rightarrow 2\pi} g_{\omega \rightarrow 3\pi} \\ g_{\omega \rightarrow 2\pi} g_{\omega \rightarrow 3\pi} & g_{\omega \rightarrow 3\pi}^2 \end{pmatrix}, \quad (2)$$

where g are the coupling constants described later. The $g_{\rho \rightarrow 3\pi}^2$ coupling is 4–5 orders of magnitude smaller than $g_{\rho \rightarrow 2\pi}^2$ [10, 29, 30] and has been neglected here. The T -matrix is obtained from $\hat{T} = [1 - iK\varrho]^{-1}K$, where the phase-space matrix ϱ is diagonal, $\varrho = \text{diag}(\varrho_{2\pi}(s), \varrho_{3\pi}(s))$, and is detailed in the supplemental material. The decay amplitude is given by

$$\mathcal{M} = \hat{A}_{2\pi} \sqrt{B_1(p_\pi)}, \quad (3)$$

where $\hat{A}_{2\pi} \equiv \alpha_{2\pi} \hat{T}_{2\pi, 2\pi} + \alpha_{3\pi} \hat{T}_{2\pi, 3\pi}$, and the elements of the production Q -vector ($\alpha_{2\pi}, \alpha_{3\pi}$) are real [31]. The coupling constants are fully determined from other experiments [10],

$$g_{\rho \rightarrow 2\pi}^2 = m_\rho \Gamma_\rho / \varrho_{2\pi}(m_\rho^2), \quad (4)$$

$$g_{\omega \rightarrow 3\pi}^2 = m_\omega \Gamma_\omega \mathcal{B}(\omega \rightarrow \pi^+\pi^-\pi^0) / \varrho_{3\pi}(m_\omega^2), \quad (5)$$

$$g_{\omega \rightarrow 2\pi}^2 = m_\omega \Gamma_\omega \mathcal{B}(\omega \rightarrow \pi^+\pi^-) / \varrho_{2\pi}(m_\omega^2). \quad (6)$$

Numerically, $g_{\omega \rightarrow 2\pi}^2 / g_{\rho \rightarrow 2\pi}^2 \approx 0.0009$, while $g_{\omega \rightarrow 2\pi} g_{\omega \rightarrow 3\pi} / g_{\rho \rightarrow 2\pi}^2 \approx 0.01$. Thus, the diagonal ω coupling to two pions can be neglected in comparison with the off-diagonal coupling. In this approximation, equivalent to the full formalism given the precision of this analysis,

$$\hat{T}_{2\pi, 2\pi} \approx \frac{g_{\rho \rightarrow 2\pi}^2}{m_\rho^2 - s - i g_{\rho \rightarrow 2\pi}^2 \varrho_{2\pi}(s)}, \quad (7)$$

which is the ρ^0 Breit–Wigner amplitude (Eq. 1) and $\alpha_{2\pi}$ is the ρ^0 production factor in the $\chi_{c1}(3872)$ decay. A mild dependence of $\alpha_{2\pi}$ on s is possible, since $\alpha_{2\pi}(s)$ must be analytic and cannot change much within the resonance widths (see *e.g.* Ref. [32]). Using Chebyshev polynomials (C_n) to express the dependence: $\alpha_{2\pi}(s) = \sum_{n=0}^{n=N} P_n C_n(\hat{s})$, where $\hat{s} \equiv 2(s - s_{\min}) / (s_{\max} - s_{\min}) - 1$, $s_{\min} = (380 \text{ MeV})^2$ and $s_{\max} = (775 \text{ MeV})^2$. The polynomial coefficients P_n are determined from a fit to the data, except for P_0 , which is set to unity as the normalization choice. For $\alpha_{2\pi}(s)$ to have the expected theoretical behavior, the series must converge, $|P_{n+1}| < |P_n|$ and N should be kept small.

The ω contribution enters via the element,

$$\hat{T}_{2\pi, 3\pi} \approx \frac{g_{\omega \rightarrow 2\pi} g_{\omega \rightarrow 3\pi} (m_\rho^2 - s)}{(m_\rho^2 - s - i g_{\rho \rightarrow 2\pi}^2 \varrho_{2\pi}(s))(m_\omega^2 - s - i g_{\omega \rightarrow 3\pi}^2 \varrho_{3\pi}(s))}. \quad (8)$$

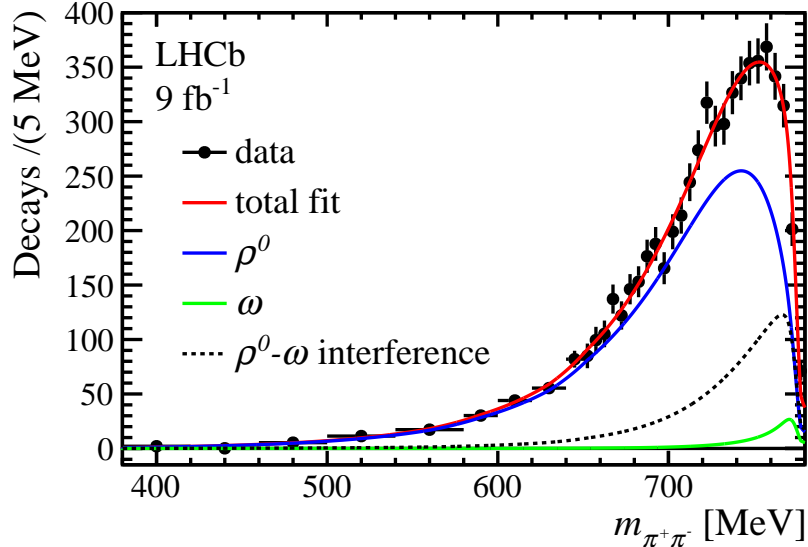


Figure 3: Distribution of $m_{\pi^+\pi^-}$ in $\chi_{c1}(3872) \rightarrow \pi^+\pi^- J/\psi$ decays, fit with the default K -matrix model.

This term approaches zero at the bare ρ^0 pole mass, which complicates probing the ω contribution, $m_\omega = 782.66 \pm 0.13$ MeV and $\Gamma_\omega = 8.68 \pm 0.13$ MeV [10]. This zero is an artifact of the K -matrix approach, rather than an expectation from scattering theory. To remove it and restore a more physical behavior of the ω term,

$$\alpha_{3\pi} = a_\omega \frac{m_\omega^2 - m_\rho^2}{m_\rho^2 - s}, \quad (9)$$

is set. The constant term $m_\omega^2 - m_\rho^2$ is introduced above to make a_ω express the ratio of ω/ρ amplitudes at the ω pole. The value of a_ω is determined by the fit to the data. Using Eqs. 7, 8 and 9, with $\alpha_{2\pi}$ constant ($N = 0$), is the common method to describe $\rho^0 - \omega$ interference in analyses of the $\pi^+\pi^-$ system [33]. The exact K -matrix formulae are used here. In view of Eq. 7, models with $\alpha_{3\pi} = 0$ are interpreted as containing a ρ^0 component only. The following integrals are calculated to quantify a relative rate of the ω contribution: $I_{\text{tot}} = \int \mathcal{P}(m_{\pi^+\pi^-}) dm_{\pi^+\pi^-}$, $I_\rho = \int \mathcal{P}(m_{\pi^+\pi^-} | \alpha_{3\pi} = 0) dm_{\pi^+\pi^-}$ and $I_\omega = \int \mathcal{P}(m_{\pi^+\pi^-} | \alpha_{2\pi} = 0) dm_{\pi^+\pi^-}$, where $\mathcal{P}(m_{\pi^+\pi^-})$ is neither convolved with the mass resolution, nor multiplied by the efficiency function. The integration is performed over the full phase space. To quantify the overall impact of ω on the total rate, including $\rho^0 - \omega$ interference effects, the ratio $\mathcal{R}_\omega^{\text{all}} \equiv 1 - I_\rho/I_{\text{tot}}$ is defined. The traditional ω fit fraction is given by $\mathcal{R}_\omega^0 \equiv I_\omega/I_{\text{tot}}$. Finally, to probe the ratio of the $\chi_{c1}(3872)$ isospin conserving to isospin violating couplings, the ratio $\mathcal{R}_{\omega/\rho}^0 \equiv I_\omega/I_\rho$ is introduced. Using the $B^+ \rightarrow K^+ \chi_{c1}(3872)$ simulation, the extraction of the dipion mass distribution and subsequent fit with the K -matrix model, with the efficiency and the mass resolution corrections included, are verified to a precision an order of magnitude better than the total systematic uncertainties reported below.

Allowing the ω term in the K -matrix model with the constant $\alpha_{2\pi}$ improves the fit quality to $\chi^2/\text{NDoF} = 55.1/33$, resulting in a significance for the ω contribution of $n_\sigma = (\chi_{a_\omega=0}^2 - \chi_{a_\omega \neq 0}^2)^{1/2} = 17.7\sigma$ [34]. However, the p -value of the fit is marginal (0.9%). Introducing a term linear in s to $\alpha_{2\pi}(s)$ improves the fit with $\chi^2/\text{NDoF} = 24.7/32$, p -value

= 82%, and a small slope coefficient, $P_1 = 0.23 \pm 0.05$. This fit, shown in Fig. 3, is taken as the default model and yields $n_\sigma = 8.1\sigma$, $\mathcal{R}_\omega^{\text{all}} = 0.214 \pm 0.023$, $\mathcal{R}_\omega^0 = 0.0193 \pm 0.0044$, $\mathcal{R}_{\omega/\rho}^0 = 0.0246 \pm 0.0062$ and $a_\omega = 0.208 \pm 0.024$. The ω contribution is at the level of $\mathcal{R}_\omega^0 \approx 2\%$ as expected from the $\chi_{c1}(3872) \rightarrow \omega J/\psi$, $\omega \rightarrow \pi^+\pi^-\pi^0$ measurements (see above). The impact on the overall $\chi_{c1}(3872) \rightarrow \pi^+\pi^- J/\psi$ rate given by $\mathcal{R}_\omega^{\text{all}}$ is an order of magnitude larger, enhanced by the $\rho^0 - \omega$ interference. Allowing a quadratic term in $\alpha_{2\pi}(s)$ lowers the p -value of the fit to 78% with $\chi^2/\text{NDoF} = 24.6/31$, indicating that too much freedom is added to the model. The P_2 coefficient is small and consistent with zero, $P_2 = 0.016 \pm 0.047$, while all other fit results remain consistent with the default fit, $P_1 = 0.21 \pm 0.07$, $\mathcal{R}_\omega^{\text{all}} = 0.206 \pm 0.035$, $\mathcal{R}_\omega^0 = 0.0178 \pm 0.0062$, $\mathcal{R}_{\omega/\rho}^0 = 0.0225 \pm 0.088$ and $a_\omega = 0.197 \pm 0.042$. The significance of the ω contribution remains very high, $n_\sigma = 5.5\sigma$, and is now underestimated, since the null hypothesis ($a_\omega = 0$) gives an unphysical polynomial correction (the quadratic term, $P_2 = 0.17 \pm 0.02$, comparable to, and more significant than the linear term, $P_1 = 0.16 \pm 0.05$).

A number of analysis variations have been performed to evaluate systematic uncertainties on the ω fraction, as summarized in Table 1. In the dipion mass extraction from the data, Gaussian functions are used for the $\chi_{c1}(3872)$ shape in $m_{\pi^+\pi^- J/\psi}$ data, rather than Crystal Ball functions. A cubic polynomial replaces the quadratic function in the relative efficiency parametrization.

Data-driven corrections to the simulation of the hadron identification are implemented, as a cross-check. To check further the relative efficiency simulation and the background subtraction, a tighter data selection is implemented with a Boosted Decision Tree (BDT) classifier [35], using inputs from hadron identification variables, the B^+ vertex quality, the PV impact parameters of the final-state particles and the B^+ candidate, the hadron transverse-momenta and the B^+ flight distance. The tighter selection reduces the combinatoric background under the B^+ peak in the $m_{K^+\pi^+\pi^- J/\psi}$ distribution from 9.4% to 3.1%, resulting in an overall background reduction under the $\chi_{c1}(3872)$ peak in the $m_{\pi^+\pi^- J/\psi}$ distribution from 23% to 17%. At the same time, the $\chi_{c1}(3872)$ signal yield is reduced by only 0.4%.

To evaluate uncertainties due to the mass resolution used in the fit, the scaling factor f_m is varied and the fit range is reduced to exclude the last interval of the $m_{\pi^+\pi^-}$ distribution (775–780 MeV), since this falls beyond the phase-space limit, and therefore its content is very sensitive to $\sigma(m_{\pi^+\pi^-})$.

To check for interference effects between $B^+ \rightarrow K^+ \chi_{c1}(3872)$ and $B^+ \rightarrow K^{*+} J/\psi$ decays, the data are split into two subsamples depending on the sign of $\cos \theta_X$, where θ_X is the $\chi_{c1}(3872)$ helicity angle, the angle between the K^+ and J/ψ momenta in the $\chi_{c1}(3872)$ rest frame. The composition of K^{*+} resonances is different in each subsample.

As a variation of the production model, non-resonant (NR) terms are added to the production vector, $(\hat{A}_{2\pi}, \hat{A}_{3\pi}) = [1 - i K \varrho]^{-1} [K(\alpha_{2\pi}, \alpha_{3\pi}) + (f_{2\pi}, f_{3\pi})]$. Without $\chi_{c1}(3872) \rightarrow 3\pi J/\psi$ data in the fit, the NR production parameter $f_{3\pi}$ cannot be probed, thus it is set to zero. A good-quality fit is obtained with constant $\alpha_{2\pi}$, which gives $f_{2\pi} = (-9.7 \pm 1.6) \times 10^{-7}$.

The default fit assumes an S -wave $\chi_{c1}(3872)$ decay. When a D -wave component is allowed in the fit, multiplying $|\mathcal{M}|^2$ by $1 + A_D^2 B_2(p_{J/\psi})/B_2(p_{J/\psi}^\rho)$, where $p_{J/\psi}^\rho \equiv p_{J/\psi}(m_\rho)$ and $B_2(p) \equiv p^4/(9 + 3(Rp)^2 + (Rp)^4)$, the A_D parameter is consistent with zero, 0.13 ± 0.41 . Tuning A_D to 0.176 produces a 4% D -wave fraction, equal to the upper limit from studies of the angular correlations [5].

Table 1: Results for ω fractions with systematic uncertainties. See text for a description of the individual entries.

Fit type	χ^2/NDof	p -value	$\mathcal{R}_\omega^{\text{all}}$	\mathcal{R}_ω^0	$\mathcal{R}_{\omega/\rho}^0$	n_σ
Default	24.7/32	0.82	0.214 ± 0.023	0.019 ± 0.004	0.025 ± 0.006	8.1σ
$P_2 \neq 0$	24.6/31	0.78	0.206 ± 0.035	0.018 ± 0.006	0.023 ± 0.009	5.5σ
Gaussian $\chi_{\text{cl}}(3872)$	20.0/32	0.95	0.194 ± 0.024	0.016 ± 0.004	0.020 ± 0.006	7.3σ
cubic $\epsilon(m_{\pi^+\pi^-})$	24.5/32	0.83	0.221 ± 0.023	0.021 ± 0.005	0.027 ± 0.007	8.1σ
had.ID corrections	24.6/32	0.82	0.214 ± 0.023	0.019 ± 0.004	0.025 ± 0.006	8.1σ
BDT selection	24.6/32	0.82	0.207 ± 0.022	0.018 ± 0.004	0.023 ± 0.006	7.9σ
$\sigma(m_{\pi^+\pi^-}) \times 1.0$	26.6/32	0.74	0.213 ± 0.023	0.019 ± 0.004	0.025 ± 0.006	8.1σ
$\sigma(m_{\pi^+\pi^-}) \times 1.14$	22.6/32	0.89	0.215 ± 0.023	0.020 ± 0.004	0.026 ± 0.006	8.1σ
$m_{\pi^+\pi^-} < 775$ MeV	18.0/31	0.97	0.196 ± 0.024	0.016 ± 0.004	0.021 ± 0.006	7.1σ
$\cos\theta_X < 0$	26.9/32	0.72	0.211 ± 0.035	0.019 ± 0.007	0.024 ± 0.010	5.2σ
$\cos\theta_X > 0$	42.2/32	0.11	0.217 ± 0.030	0.021 ± 0.006	0.027 ± 0.009	4.2σ
NR prod. of 2π	24.7/32	0.82	0.214 ± 0.022	0.019 ± 0.004	0.025 ± 0.006	8.1σ
D -wave free	24.5/31	0.79	0.210 ± 0.029	0.017 ± 0.005	0.021 ± 0.007	7.8σ
D -wave fixed at 4%	24.5/32	0.82	0.208 ± 0.023	0.018 ± 0.004	0.023 ± 0.006	7.9σ
ρ'	25.1/32	0.80	0.209 ± 0.023	0.018 ± 0.004	0.024 ± 0.006	8.1σ
$R_{\text{prod}} = 0$ GeV $^{-1}$	24.7/32	0.82	0.209 ± 0.023	0.019 ± 0.004	0.024 ± 0.006	7.9σ
$R_{\text{prod}} = 30$ GeV $^{-1}$	24.6/32	0.82	0.229 ± 0.022	0.021 ± 0.004	0.028 ± 0.006	8.7σ
$R = 1.3$ GeV $^{-1}$	24.7/32	0.82	0.216 ± 0.022	0.020 ± 0.004	0.026 ± 0.006	8.2σ
$R = 1.6$ GeV $^{-1}$	24.7/32	0.82	0.212 ± 0.023	0.019 ± 0.004	0.025 ± 0.006	8.0σ
GS model	24.8/32	0.81	0.221 ± 0.024	0.021 ± 0.005	0.028 ± 0.007	7.8σ
Summary			$0.214 \pm 0.023 \pm 0.020$	$0.019 \pm 0.004 \pm 0.003$	$0.025 \pm 0.006 \pm 0.005$	$> 7.1\sigma$

Since the hadron size parameter R is tuned to the scattering data, which automatically includes any ρ^0 excitations, there is no strong motivation to include the $\rho(1450)$ pole [10] (ρ') in the K -matrix model. When included, the fit quality is slightly reduced.

The size parameter R used in $B_1(p_\pi)$ of Eq. 3 could be related to the $\chi_{\text{cl}}(3872)$ size, rather than the ρ^0 or ω sizes. Thus, fit variations are tried in which it has an independent value, R_{prod} , varied from zero to 30 GeV^{-1} . The R value itself is varied within the range 1.3 – 1.6 GeV^{-1} . An alternative model of the ρ^0 shape, that does not include an R -dependent Blatt–Weisskopf form factor, is provided by the Gounaris–Sakurai (GS) formula [36], and was utilized by the BaBar collaboration to describe high statistics $e^+e^- \rightarrow \pi^+\pi^-(\gamma)$ data [37]. As discussed in the supplemental material, when applying this prescription with ρ^0 , ρ' and ω contributions, an excellent fit to the data is obtained, $\chi^2/\text{NDof} = 24.8/32$, p -value = 81%, matching the fit quality of the default fit.

Total systematic uncertainties, given at the bottom of Table 1, are set to cover the maximal deviation from the default fit results, and are comparable to the statistical uncertainties. The lowest ω significance is 7.1σ , excluding the subsamples and $P_2 \neq 0$ fit as discussed above. This is a more significant observation of $\chi_{\text{cl}}(3872) \rightarrow \omega J/\psi$ decays than achieved using the dominant $\omega \rightarrow \pi^+\pi^-\pi^0$ decay channel.

In addition to the resonant coupling constants, the limited phase space in $\chi_{c1}(3872) \rightarrow \pi^+\pi^- J/\psi$ decays has a large impact on the $\mathcal{R}_{\omega/\rho}^0$ value capturing a much smaller fraction of the ω resonance than for the ρ^0 resonance. To probe the resonant coupling constants, the phase space can be artificially extended to contain both resonance peaks by setting $m_{\chi_{c1}(3872)} = 4000$ MeV, as illustrated in the supplemental material. Integrating the default $\mathcal{P}(m_{\pi^+\pi^-})$ model in the extended phase space, $\mathcal{R}_{\omega/\rho}^0 = 0.18 \pm 0.05$ is obtained and then used to deduce the ratio of the isospin violating to isospin conserving $\chi_{c1}(3872)$ couplings,

$$\frac{g_{\chi_{c1}(3872) \rightarrow \rho^0 J/\psi}}{g_{\chi_{c1}(3872) \rightarrow \omega J/\psi}} = \sqrt{\frac{\mathcal{B}(\omega \rightarrow \pi^+\pi^-)}{\mathcal{R}_{\omega/\rho}^0}} = 0.29 \pm 0.04.$$

This value is an order of magnitude larger than expected for pure $c\bar{c}$ states, as exemplified by the corresponding value for the $\psi(2S)$ state [10],

$$\frac{g_{\psi(2S) \rightarrow \pi^0 J/\psi}}{g_{\psi(2S) \rightarrow \eta J/\psi}} = \sqrt{\frac{\mathcal{B}(\psi(2S) \rightarrow \pi^0 J/\psi)}{\mathcal{B}(\psi(2S) \rightarrow \eta J/\psi)}} \frac{p_\eta^3}{p_{\pi^0}^3} = 0.045 \pm 0.001,$$

where p_η and p_{π^0} are the breakup momenta [38]. Therefore, the $\chi_{c1}(3872)$ state cannot be a pure charmonium state. Large isospin violation is naturally expected in models in which the $\chi_{c1}(3872)$ state has a significant $D\bar{D}^*$ component, either as constituents (*i.e.* in the ‘‘molecular model’’) or generated dynamically in the decay [39–48]. The proximity of the $\chi_{c1}(3872)$ mass to the $D^0\bar{D}^{*0}$ threshold, enhances such contributions over D^+D^{*-} combinations, which are 8 MeV heavier. It has also been suggested in compact tetraquark models that two neutral states could be degenerate and mix, giving rise to large isospin violation in $\chi_{c1}(3872)$ decays [49–51].

In summary, the ρ^0 and ω contributions to $\chi_{c1}(3872) \rightarrow \pi^+\pi^- J/\psi$ decays are resolved for the first time using a much larger data sample than previously available. Through $\rho^0 - \omega$ interference, the ω contribution accounts for $(21.4 \pm 2.3 \pm 2.0)\%$ of the total rate, or equivalently, $\mathcal{B}(\chi_{c1}(3872) \rightarrow \rho^0 J/\psi)/\mathcal{B}(\chi_{c1}(3872) \rightarrow \pi^+\pi^- J/\psi) = (78.6 \pm 2.3 \pm 2.0)\%$. Excluding interference effects, the ω contribution, $(1.9 \pm 0.4 \pm 0.3)\%$, is found to be consistent with, but more precise than the previous $\chi_{c1}(3872) \rightarrow \omega J/\psi$ measurements utilizing $\omega \rightarrow \pi^+\pi^-\pi^0$ decays [9, 11, 12]. The isospin violating ρ^0 contribution, quantified for the first time with proper subtraction of the ω contribution, is an order of magnitude too large for $\chi_{c1}(3872)$ to be a pure charmonium state.

This analysis also serves as an excellent illustration for why a simple sum of ρ^0 and ω Breit–Wigner amplitudes should not be used to describe interfering resonances. Such a model fails to describe the data, while the K -matrix approach, which respects unitarity, provides an excellent description of the data and gives numerical results that are consistent with the previous $\chi_{c1}(3872) \rightarrow \omega J/\psi$ measurements utilizing $\omega \rightarrow \pi^+\pi^-\pi^0$ decays.

Acknowledgements

We express our gratitude to our colleagues in the CERN accelerator departments for the excellent performance of the LHC. We thank the technical and administrative staff at the LHCb institutes. We acknowledge support from CERN and from the national agencies: CAPES, CNPq, FAPERJ and FINEP (Brazil); MOST and NSFC (China); CNRS/IN2P3

(France); BMBF, DFG and MPG (Germany); INFN (Italy); NWO (Netherlands); MNiSW and NCN (Poland); MEN/IFA (Romania); MICINN (Spain); SNSF and SER (Switzerland); NASU (Ukraine); STFC (United Kingdom); DOE NP and NSF (USA). We acknowledge the computing resources that are provided by CERN, IN2P3 (France), KIT and DESY (Germany), INFN (Italy), SURF (Netherlands), PIC (Spain), GridPP (United Kingdom), CSCS (Switzerland), IFIN-HH (Romania), CBPF (Brazil), Polish WLCG (Poland) and NERSC (USA). We are indebted to the communities behind the multiple open-source software packages on which we depend. Individual groups or members have received support from ARC and ARDC (Australia); Minciencias (Colombia); AvH Foundation (Germany); EPLANET, Marie Skłodowska-Curie Actions and ERC (European Union); A*MIDEX, ANR, IPhU and Labex P2IO, and Région Auvergne-Rhône-Alpes (France); Key Research Program of Frontier Sciences of CAS, CAS PIFI, CAS CCEPP, Fundamental Research Funds for the Central Universities, and Sci. & Tech. Program of Guangzhou (China); MEFP, GVA, XuntaGal, GENCAT and Prog. Atracción Talento, CM (Spain); SRC (Sweden); the Leverhulme Trust, the Royal Society and UKRI (United Kingdom).

Observation of sizeable ω contribution to $\chi_{c1}(3872) \rightarrow \pi^+ \pi^- J/\psi$ decays

Supplemental material

1 K -matrix phase-space matrix elements

A notation in which the Blatt–Weisskopf barrier factors (B_l) are integrated with the phase-space matrix is used in this Letter,

$$\varrho_{2\pi}(s) = \frac{2p_\pi}{\sqrt{s}} B_1(p_\pi). \quad (\text{S1})$$

Since the ω meson decays to three pions via a P -wave $\rho\pi$ decay,

$$\varrho_{3\pi}(s) = \int_{(2m_\pi)^2}^{(\sqrt{s}-m_\pi)^2} d\sigma \frac{2p_\pi(\sigma)}{\sqrt{\sigma}} \frac{B_1(p_\pi(\sigma))}{(m_\rho^2 - \sigma)^2 + (m_\rho \Gamma_\rho)^2} \frac{2p'_3(s, \sigma)}{\sqrt{s}} B_1(p'_3(s, \sigma)) \quad (\text{S2})$$

$$p'_3(s, \sigma) = \frac{\sqrt{(s - (\sqrt{\sigma} + m_\pi)^2)(s - (\sqrt{\sigma} - m_\pi)^2)}}{2\sqrt{s}}. \quad (\text{S3})$$

2 Gounaris–Sakurai resonant $m_{\pi^+\pi^-}$ shape

An alternative model to the R -dependent Blatt–Weisskopf form factor in the Breit–Wigner amplitude is provided by the Gounaris–Sakurai formula [36],

$$\text{BW}_\rho^{\text{GS}}(s | m_\rho, \Gamma_\rho) = \frac{m_\rho^2 [1 + d(m_\rho)\Gamma_\rho/m_\rho]}{m_\rho^2 - s + f(s, m_\rho, \Gamma_\rho) - i m_\rho \Gamma(s, m_\rho, \Gamma_\rho)}, \quad (\text{S4})$$

where,

$$\Gamma(s, m, \Gamma_0) = \Gamma_0 \frac{m}{\sqrt{s}} \left[\frac{p_\pi(s)}{p_\pi(m^2)} \right]^3, \quad (\text{S5})$$

$$d(m) = \frac{3}{\pi} \frac{m_\pi^2}{p_\pi^2(m^2)} \log \left[\frac{m + 2p_\pi(m^2)}{2m_\pi} \right] + \frac{m}{2\pi p_\pi(m^2)} - \frac{m_\pi^2 m}{\pi p_\pi^3(m^2)}, \quad (\text{S6})$$

$$f(s, m, \Gamma_0) = \frac{\Gamma_0 m^2}{p_\pi^3(m^2)} [p_\pi^2(s) [h(s) - h(m^2)] + (m^2 - s) p_\pi^2(m^2) h'(m^2)], \quad (\text{S7})$$

$$h(s) = \frac{2}{\pi} \frac{p_\pi(s)}{\sqrt{s}} \log \left[\frac{\sqrt{s} + 2p_\pi(s)}{2m_\pi} \right], \quad (\text{S8})$$

and $h'(s)$ is the derivative of $h(s)$, with respect to s , calculated numerically. To include the P -wave momentum barrier in the ρ^0 decay, the matrix element is set to $\mathcal{M} = p_\pi(s)/p_\pi(m_\rho) \text{BW}_\rho^{\text{GS}}(s, m_\rho, \Gamma_\rho)$. A fit of this ρ^0 shape to the data is only slightly

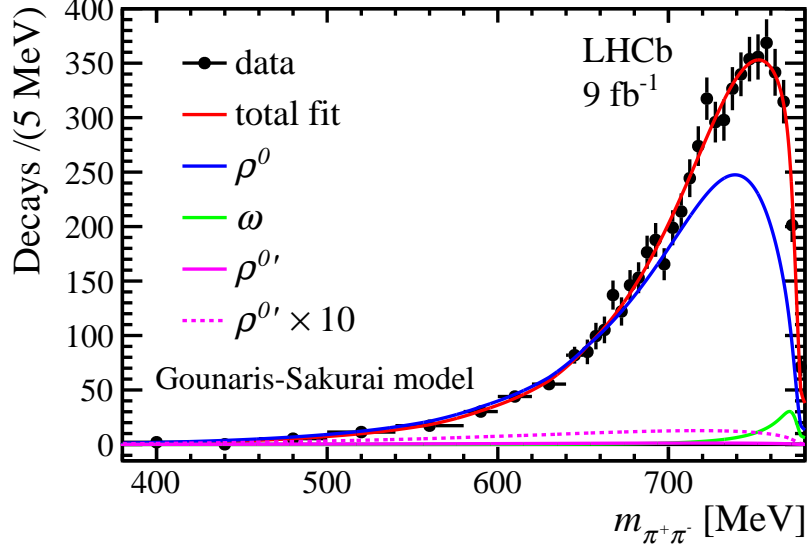


Figure S1: Distribution of $m_{\pi^+\pi^-}$ in $\chi_{c1}(3872) \rightarrow \pi^+\pi^- J/\psi$ decays, fit with the Gounaris–Sakurai model. The dashed line represents the ρ' contribution multiplied by a factor of 10.

better than the fit of the Breit–Wigner shape given by Eq. 1 ($\chi^2/\text{NDoF} = 290.0/34$, $p\text{-value} = 2 \times 10^{-42}$). A good-quality fit to the data is achieved following the prescription used by the BaBar collaboration to describe a large $e^+e^- \rightarrow \pi^+\pi^-(\gamma)$ data sample [37],

$$\mathcal{M} = \frac{p_\pi(s)}{p_\pi(m_\rho)} \left\{ \text{BW}^{\text{GS}}(s, m_\rho, \Gamma_\rho) [1 + A_\omega^{\text{GS}} e^{i\phi_\omega} \text{BW}_\omega(s, m_\omega, \Gamma_\omega)] \right. \quad (\text{S9}) \\ \left. + A_{\rho'}^{\text{GS}} e^{i\phi_{\rho'}} \text{BW}^{\text{GS}}(s, m_{\rho'}, \Gamma_{\rho'}) \right\}.$$

Following this work, a simple Breit–Wigner amplitude for the ω meson is used, $\text{BW}_\omega(s, m_\omega, \Gamma_\omega) = m_\omega^2 / (m_\omega^2 - s - im_\omega\Gamma_\omega)$, and the ρ^0 , ω and ρ' masses and widths are taken from Table VI of Ref. [37]. The term including the ρ^0 and ω resonances (Eq. S9) is equivalent to Eqs. 8-9, and thus originates from the coupled-channel approach. No complex phase is expected in this approach, thus ϕ_ω is set to zero. Using the small phase, consistent with zero, obtained by the BaBar collaboration, gives almost identical results. Since, the ρ' contribution is not added via the K -matrix, its phase can be different from zero and is fixed to the central value of the BaBar result, $\phi_{\rho'} = 3.76 \pm 0.10$ rad. The $m_{\pi^+\pi^-}$ distribution, fit with this model, is shown in Fig. S1. The fit quality is excellent ($\chi^2/\text{NDoF} = 24.8/32$, $p\text{-value} = 0.81$), matching the fit quality of the default fit. The ρ' significance is 3.1σ using Wilks' theorem [34]. Its production parameter relative to the ρ^0 meson, $A_{\rho'}^{\text{GS}} = 0.302 \pm 0.099$, is consistent within the large uncertainty with the value obtained by the fit to the BaBar data, 0.158 ± 0.018 [37]. The ω significance is 7.8σ , and its production parameter, $A_\omega^{\text{GS}} = 0.0171 \pm 0.0024$, is an order of magnitude larger than that obtained by the BaBar collaboration, 0.001644 ± 0.00061 [37]. This is not surprising, since in e^+e^- collisions, the ρ^0 meson is produced via electromagnetic interactions, which do not follow isospin symmetry, while in $\chi_{c1}(3872)$ decays, the ρ^0 state is produced via strong interactions, which suppress isospin violating decays. The ω fractional contributions are consistent with the default model, $\mathcal{R}_\omega^{\text{all}} = 0.221 \pm 0.024$, $\mathcal{R}_\omega^0 = 0.021 \pm 0.005$ and $\mathcal{R}_{\omega/\rho}^0 = 0.028 \pm 0.007$. Here, $\mathcal{R}_\omega^{\text{all}} = 1 - \mathcal{R}_{\rho+\rho'}$, where $\mathcal{R}_{\rho+\rho'} = 0.780 \pm 0.023$ is the

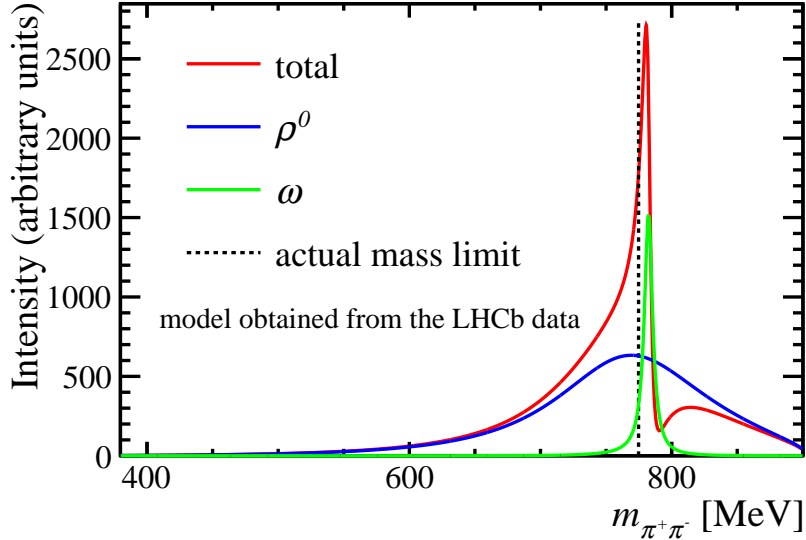


Figure S2: Amplitude model for $\chi_{c1}(3872) \rightarrow \pi^+\pi^- J/\psi$ decays, obtained by the default fit to the LHCb data (Fig. 3), with the phase-space integration limit extended by setting the $\chi_{c1}(3872)$ mass to 4000 MeV. The actual phase-space limit, imposed by the measured $\chi_{c1}(3872)$ mass, is indicated by the vertical dashed line. Neither mass resolution nor detector efficiency are applied here.

coherent fit fraction of the ρ^0 and $\rho^{0'}$ contributions together. The individual fit fractions are $\mathcal{R}_\rho = 0.833 \pm 0.037$ and $\mathcal{R}_{\rho'} = 0.013 \pm 0.008$.

3 Extended $\chi_{c1}(3872) \rightarrow \pi^+\pi^- J/\psi$ decay phase space

To estimate the ratio of the isospin violating to isospin conserving $\chi_{c1}(3872)$ couplings, the mass of the $\chi_{c1}(3872)$ state in the model obtained by the default fit to the dipion mass distribution is replaced by 4000 MeV. The extended decay phase space is integrated over both the ρ^0 and ω resonant peaks, as illustrated in Fig. S2. The obtained ratio, $g_{\chi_{c1}(3872) \rightarrow \rho^0 J/\psi} / g_{\chi_{c1}(3872) \rightarrow \omega J/\psi} = 0.29 \pm 0.04$, is an order of magnitude larger than the value for the well established charmonium state, $g_{\psi(2S) \rightarrow \pi^0 J/\psi} / g_{\psi(2S) \rightarrow \eta J/\psi} = 0.045 \pm 0.001$.

References

- [1] Belle collaboration, S. K. Choi *et al.*, *Observation of a narrow charmonium-like state in exclusive $B^\pm \rightarrow K^\pm \pi^+ \pi^- J/\psi$ decays*, Phys. Rev. Lett. **91** (2003) 262001, arXiv:hep-ex/0309032.
- [2] BaBar collaboration, B. Aubert *et al.*, *Search for a charged partner of the $X(3872)$ in the B meson decay $B \rightarrow X^- K$, $X^- \rightarrow J/\psi \pi^- \pi^0$* , Phys. Rev. **D71** (2005) 031501, arXiv:hep-ex/0412051.
- [3] Belle collaboration, S.-K. Choi *et al.*, *Bounds on the width, mass difference and other properties of $X(3872) \rightarrow \pi^+ \pi^- J/\psi$ decays*, Phys. Rev. **D84** (2011) 052004, arXiv:1107.0163.
- [4] LHCb collaboration, R. Aaij *et al.*, *Determination of the $X(3872)$ meson quantum numbers*, Phys. Rev. Lett. **110** (2013) 222001, arXiv:1302.6269.
- [5] LHCb collaboration, R. Aaij *et al.*, *Quantum numbers of the $X(3872)$ state and orbital angular momentum in its $\rho^0 J/\psi$ decays*, Phys. Rev. **D92** (2015) 011102(R), arXiv:1504.06339, and supplementary material.
- [6] E. Eichten *et al.*, *Charmonium: The model*, Phys. Rev. **D17** (1978) 3090, [Erratum: Phys.Rev.D 21, 313 (1980)].
- [7] S. L. Olsen, T. Skwarnicki, and D. Zieminska, *Nonstandard heavy mesons and baryons: Experimental evidence*, Rev. Mod. Phys. **90** (2018) 015003, arXiv:1708.04012.
- [8] F.-K. Guo *et al.*, *Hadronic molecules*, Rev. Mod. Phys. **90** (2018) 015004, arXiv:1705.00141.
- [9] BESIII collaboration, M. Ablikim *et al.*, *Study of $e^+e^- \rightarrow \gamma \omega J/\psi$ and observation of $X(3872) \rightarrow \omega J/\psi$* , Phys. Rev. Lett. **122** (2019) 232002, arXiv:1903.04695.
- [10] Particle Data Group, P. A. Zyla *et al.*, *Review of particle physics*, Prog. Theor. Exp. Phys. **2020** (2020) 083C01.
- [11] Belle collaboration, K. Abe *et al.*, *Evidence for $X(3872) \rightarrow \gamma J/\psi$ and the sub-threshold decay $X(3872) \rightarrow \omega J/\psi$* , in *Lepton and photon interactions at high energies. Proceedings, 22nd International Symposium, LP 2005, Uppsala, Sweden, June 30-July 5, 2005*, 2005, arXiv:hep-ex/0505037.
- [12] BaBar collaboration, P. del Amo Sanchez *et al.*, *Evidence for the decay $X(3872) \rightarrow J/\psi \omega$* , Phys. Rev. **D82** (2010) 011101, arXiv:1005.5190.
- [13] CDF collaboration, A. Abulencia *et al.*, *Measurement of the dipion mass spectrum in $X(3872) \rightarrow J/\psi \pi^+ \pi^-$ decays*, Phys. Rev. Lett. **96** (2006) 102002, arXiv:hep-ex/0512074.
- [14] LHCb collaboration, A. A. Alves Jr. *et al.*, *The LHCb detector at the LHC*, JINST **3** (2008) S08005.

- [15] LHCb collaboration, R. Aaij *et al.*, *LHCb detector performance*, Int. J. Mod. Phys. **A30** (2015) 1530022, arXiv:1412.6352.
- [16] W. D. Hulsbergen, *Decay chain fitting with a Kalman filter*, Nucl. Instrum. Meth. **A552** (2005) 566, arXiv:physics/0503191.
- [17] T. Skwarnicki, *A study of the radiative cascade transitions between the Upsilon-prime and Upsilon resonances*, PhD thesis, Institute of Nuclear Physics, Krakow, 1986, DESY-F31-86-02.
- [18] T. Sjöstrand, S. Mrenna, and P. Skands, *A brief introduction to PYTHIA 8.1*, Comput. Phys. Commun. **178** (2008) 852, arXiv:0710.3820; T. Sjöstrand, S. Mrenna, and P. Skands, *PYTHIA 6.4 physics and manual*, JHEP **05** (2006) 026, arXiv:hep-ph/0603175.
- [19] I. Belyaev *et al.*, *Handling of the generation of primary events in Gauss, the LHCb simulation framework*, J. Phys. Conf. Ser. **331** (2011) 032047.
- [20] D. J. Lange, *The EvtGen particle decay simulation package*, Nucl. Instrum. Meth. **A462** (2001) 152.
- [21] N. Davidson, T. Przedzinski, and Z. Was, *PHOTOS interface in C++: Technical and physics documentation*, Comp. Phys. Comm. **199** (2016) 86, arXiv:1011.0937.
- [22] Geant4 collaboration, J. Allison *et al.*, *Geant4 developments and applications*, IEEE Trans. Nucl. Sci. **53** (2006) 270; Geant4 collaboration, S. Agostinelli *et al.*, *Geant4: A simulation toolkit*, Nucl. Instrum. Meth. **A506** (2003) 250.
- [23] M. Clemencic *et al.*, *The LHCb simulation application, Gauss: Design, evolution and experience*, J. Phys. Conf. Ser. **331** (2011) 032023.
- [24] D. Müller, M. Clemencic, G. Corti, and M. Gersabeck, *ReDecay: A novel approach to speed up the simulation at LHCb*, Eur. Phys. J. **C78** (2018) 1009, arXiv:1810.10362.
- [25] R. Garcia-Martin *et al.*, *Pion-pion scattering amplitude. IV. Improved analysis with once subtracted Roy-like equations up to 1100 MeV*, Phys. Rev. **D83** (2011) 074004, arXiv:1102.2183.
- [26] CMS collaboration, S. Chatrchyan *et al.*, *Measurement of the $X(3872)$ production cross section via decays to $J/\psi\pi^+\pi^-$ in pp collisions at $\sqrt{s} = 7$ TeV*, JHEP **04** (2013) 154, arXiv:1302.3968.
- [27] ATLAS collaboration, M. Aaboud *et al.*, *Measurements of $\psi(2S)$ and $X(3872) \rightarrow J/\psi\pi^+\pi^-$ production in pp collisions at $\sqrt{s} = 8$ TeV with the ATLAS detector*, JHEP **01** (2017) 117, arXiv:1610.09303.
- [28] I. J. R. Aitchison, *K-matrix formalism for overlapping resonances*, Nucl. Phys. A **189** (1972) 417.
- [29] M. N. Achasov *et al.*, *Study of the process $e^+e^- \rightarrow \pi^+\pi^-\pi^0$ in the energy region \sqrt{s} below 0.98 GeV*, Phys. Rev. **D68** (2003) 052006, arXiv:hep-ex/0305049.

- [30] M. Benayoun, P. David, L. DelBuono, and O. Leitner, *A global treatment of VMD physics up to the ϕ : I. e^+e^- annihilations, anomalies and vector meson partial widths*, Eur. Phys. J. **C65** (2010) 211, [arXiv:0907.4047](#).
- [31] S. U. Chung *et al.*, *Partial wave analysis in K matrix formalism*, Annalen Phys. **4** (1995) 404.
- [32] JPAC/COMPASS collaboration, A. Jackura *et al.*, *New analysis of $\eta\pi$ tensor resonances measured at the COMPASS experiment*, Phys. Lett. **B779** (2018) 464, [arXiv:1707.02848](#).
- [33] A. S. Goldhaber, G. C. Fox, and C. Quigg, *Theory of $\rho - \omega$ interference in $\pi^+\pi^-$ production*, Phys. Lett. **B30** (1969) 249.
- [34] S. S. Wilks, *The large-sample distribution of the likelihood ratio for testing composite hypotheses*, Ann. Math. Stat. **9** (1938) 60.
- [35] H. Voss, A. Hoecker, J. Stelzer, and F. Tegenfeldt, *TMVA - toolkit for multivariate data analysis with ROOT*, PoS **ACAT** (2007) 040.
- [36] G. J. Gounaris and J. J. Sakurai, *Finite-width corrections to the vector meson dominance prediction for $\rho \rightarrow e^+e^-$* , Phys. Rev. Lett. **21** (1968) 244.
- [37] BaBar collaboration, J. P. Lees *et al.*, *Precise measurement of the $e^+e^- \rightarrow \pi^+\pi^-(\gamma)$ cross section with the initial-state radiation method at BABAR*, Phys. Rev. **D86** (2012) 032013, [arXiv:1205.2228](#).
- [38] C. Hanhart, Y. S. Kalashnikova, A. E. Kudryavtsev, and A. V. Nefediev, *Remarks on the quantum numbers of $X(3872)$ from the invariant mass distributions of the $\rho J/\psi$ and $\omega J/\psi$ final states*, Phys. Rev. **D85** (2012) 011501, [arXiv:1111.6241](#).
- [39] N. A. Törnqvist, *Comment on the narrow charmonium state of Belle at 3871.8 MeV as a deuson*, [arXiv:hep-ph/0308277](#).
- [40] N. A. Törnqvist, *Isospin breaking of the narrow charmonium state of Belle at 3872 MeV as a deuson*, Phys. Lett. **B590** (2004) 209, [arXiv:hep-ph/0402237](#).
- [41] M. B. Voloshin, *Interference and binding effects in decays of possible molecular component of $X(3872)$* , Phys. Lett. **B579** (2004) 316, [arXiv:hep-ph/0309307](#).
- [42] E. S. Swanson, *Short range structure in the $X(3872)$* , Phys. Lett. **B588** (2004) 189, [arXiv:hep-ph/0311229](#).
- [43] M. Suzuki, *The $X(3872)$ boson: molecule or charmonium*, Phys. Rev. **D72** (2005) 114013, [arXiv:hep-ph/0508258](#).
- [44] S. Coito, G. Rupp, and E. van Beveren, *Delicate interplay between the D^0D^{*0} , $\rho^0 J/\psi$, and $\omega J/\psi$ channels in the $X(3872)$ resonance*, Eur. Phys. J. **C71** (2011) 1762, [arXiv:1008.5100](#).
- [45] N. Li and S.-L. Zhu, *Isospin breaking, coupled-channel effects and diagnosis of $X(3872)$* , Phys. Rev. **D86** (2012) 074022, [arXiv:1207.3954](#).

- [46] S. Takeuchi, K. Shimizu, and M. Takizawa, *On the origin of the narrow peak and the isospin symmetry breaking of the $X(3872)$* , PTEP **2014** (2014) 123D01, arXiv:1408.0973, [Erratum: PTEP 2015, 079203 (2015)].
- [47] Q. Wu, D.-Y. Chen, and T. Matsuki, *A phenomenological analysis on isospin-violating decay of $X(3872)$* , Eur. Phys. J. **C81** (2021) 193, arXiv:2102.08637.
- [48] L. Meng, G.-J. Wang, B. Wang, and S.-L. Zhu, *Revisit the isospin violating decays of $X(3872)$* , Phys. Rev. **D104** (2021) 094003, arXiv:2109.01333.
- [49] K. Terasaki, *A new tetra-quark interpretation of $X(3872)$* , Prog. Theor. Phys. **118** (2007) 821, arXiv:0706.3944.
- [50] L. Maiani, A. D. Polosa, and V. Riquer, *A theory of X and Z multiquark resonances*, Phys. Lett. **B778** (2018) 247, arXiv:1712.05296.
- [51] L. Maiani, A. D. Polosa, and V. Riquer, *$X(3872)$ tetraquarks in B and B_s decays*, Phys. Rev. **D102** (2020) 034017, arXiv:2005.08764.

LHCb collaboration

R. Aaij³², A.S.W. Abdelmotteleb⁵⁰, C. Abellan Beteta⁴⁴, F. Abudinén⁵⁰,
T. Ackernley⁵⁴, B. Adeva⁴⁰, M. Adinolfi⁴⁸, H. Afsharnia⁹, C. Agapopoulou¹³,
C.A. Aidala⁷⁷, S. Aiola²⁵, Z. Ajaltouni⁹, S. Akar⁵⁹, K. Akiba³², J. Albrecht¹⁵,
F. Alessio⁴², M. Alexander⁵³, A. Alfonso Albero³⁹, Z. Aliouche⁵⁶,
P. Alvarez Cartelle⁴⁹, S. Amato², J.L. Amey⁴⁸, Y. Amhis¹¹, L. An⁴²,
L. Anderlini²², M. Andersson⁴⁴, A. Andreianov³⁸, M. Andreotti²¹, D. Ao⁶,
F. Archilli¹⁷, A. Artamonov³⁸, M. Artuso⁶², K. Arzymatov³⁸, E. Aslanides¹⁰,
M. Atzeni⁴⁴, B. Audurier¹², S. Bachmann¹⁷, M. Bachmayer⁴³, J.J. Back⁵⁰,
A. Bailly-reyre¹³, P. Baladron Rodriguez⁴⁰, V. Balagura¹², W. Baldini²¹,
J. Baptista de Souza Leite¹, M. Barbetti^{22,j}, R.J. Barlow⁵⁶, S. Barsuk¹¹,
W. Barter⁵⁵, M. Bartolini⁴⁹, F. Baryshnikov³⁸, J.M. Basels¹⁴, G. Bassi^{29,r},
B. Batsukh⁴, A. Battig¹⁵, A. Bay⁴³, A. Beck⁵⁰, M. Becker¹⁵, F. Bedeschi²⁹,
I.B. Bediaga¹, A. Beiter⁶², V. Belavin³⁸, S. Belin²⁷, V. Bellee⁴⁴, K. Belous³⁸,
I. Belov³⁸, I. Belyaev³⁸, G. Bencivenni²³, E. Ben-Haim¹³, A. Berezhniov³⁸,
R. Bernet⁴⁴, D. Berninghoff¹⁷, H.C. Bernstein⁶², C. Bertella⁵⁶, A. Bertolin²⁸,
C. Betancourt⁴⁴, F. Betti⁴², I.a. Bezshyiko⁴⁴, S. Bhasin⁴⁸, J. Bhom³⁵, L. Bian⁶⁷,
M.S. Bieker¹⁵, N.V. Biesuz²¹, S. Bifani⁴⁷, P. Billoir¹³, A. Biolchini³², M. Birch⁵⁵,
F.C.R. Bishop⁴⁹, A. Bitadze⁵⁶, A. Bizzeti⁴⁹, M. Bjørn⁵⁷, M.P. Blago⁴⁹, T. Blake⁵⁰,
F. Blanc⁴³, S. Blusk⁶², D. Bobulska⁵³, J.A. Boelhauve¹⁵, O. Boente Garcia⁴⁰,
T. Boettcher⁵⁹, A. Boldyrev³⁸, N. Bondar^{38,42}, S. Borghi⁵⁶, M. Borisyak³⁸,
M. Borsato¹⁷, J.T. Borsuk³⁵, S.A. Bouchiba⁴³, T.J.V. Bowcock^{54,42}, A. Boyer⁴²,
C. Bozzi²¹, M.J. Bradley⁵⁵, S. Braun⁶⁰, A. Brea Rodriguez⁴⁰, J. Brodzicka³⁵,
A. Brossa Gonzalo⁵⁰, D. Brundu²⁷, A. Buonaura⁴⁴, L. Buonincontri²⁸,
A.T. Burke⁵⁶, C. Burr⁴², A. Bursche⁶⁶, A. Butkevich³⁸, J.S. Butter³²,
J. Buytaert⁴², W. Byczynski⁴², S. Cadeddu²⁷, H. Cai⁶⁷, R. Calabrese^{21,i},
L. Calefice^{15,13}, S. Cali²³, R. Calladine⁴⁷, M. Calvi^{26,n}, M. Calvo Gomez⁷⁵,
P. Camargo Magalhaes⁴⁸, P. Campana²³, A.F. Campoverde Quezada⁶, S. Capelli^{26,n},
L. Capriotti^{20,g}, A. Carbone^{20,g}, G. Carboni³¹, R. Cardinale^{24,k}, A. Cardini²⁷,
I. Carli⁴, P. Carniti^{26,n}, L. Carus¹⁴, A. Casais Vidal⁴⁰, R. Caspary¹⁷, G. Casse⁵⁴,
M. Cattaneo⁴², G. Cavallero⁴², V. Cavallini^{21,i}, S. Celani⁴³, J. Cerasoli¹⁰,
D. Cervenkov⁵⁷, A.J. Chadwick⁵⁴, M.G. Chapman⁴⁸, M. Charles¹³,
Ph. Charpentier⁴², C.A. Chavez Barajas⁵⁴, M. Chefdeville⁸, C. Chen³, S. Chen⁴,
A. Chernov³⁵, V. Chobanova⁴⁰, S. Cholak⁴³, M. Chrzasczcz³⁵, A. Chubykin³⁸,
V. Chulikov³⁸, P. Ciambrone²³, M.F. Cicala⁵⁰, X. Cid Vidal⁴⁰, G. Ciezarek⁴²,
G. Ciullo^{i,21}, P.E.L. Clarke⁵², M. Clemencic⁴², H.V. Cliff⁴⁹, J. Closier⁴²,
J.L. Cobbledick⁵⁶, V. Coco⁴², J.A.B. Coelho¹¹, J. Cogan¹⁰, E. Cogneras⁹,
L. Cojocariu³⁷, P. Collins⁴², T. Colombo⁴², L. Congedo^{19,f}, A. Contu²⁷,
N. Cooke⁴⁷, G. Coombs⁵³, I. Corredoira⁴⁰, G. Corti⁴², C.M. Costa Sobral⁵⁰,
B. Couturier⁴², D.C. Craik⁵⁸, J. Crkovská⁶¹, M. Cruz Torres^{1,e}, R. Currie⁵²,
C.L. Da Silva⁶¹, S. Dadabaev³⁸, L. Dai⁶⁵, E. Dall'Occo¹⁵, J. Dalseno⁴⁰,
C. D'Ambrosio⁴², A. Danilina³⁸, P. d'Argent⁴², J.E. Davies⁵⁶, A. Davis⁵⁶,
O. De Aguiar Francisco⁵⁶, J. de Boer⁴², K. De Bruyn⁷³, S. De Capua⁵⁶,
M. De Cian⁴³, U. De Freitas Carneiro Da Graca¹, E. De Lucia²³, J.M. De Miranda¹,
L. De Paula², M. De Serio^{19,f}, D. De Simone⁴⁴, P. De Simone²³, F. De Vellis¹⁵,
J.A. de Vries⁷⁴, C.T. Dean⁶¹, F. Debernardis^{19,f}, D. Decamp⁸, V. Dedu¹⁰,
L. Del Buono¹³, B. Delaney⁴⁹, H.-P. Dembinski¹⁵, V. Denysenko⁴⁴, O. Deschamps⁹,
F. Dettori^{27,h}, B. Dey⁷¹, A. Di Cicco²³, P. Di Nezza²³, S. Didenko³⁸,
L. Dieste Maronas⁴⁰, H. Dijkstra⁴², V. Dobishuk⁴⁶, C. Dong³, A.M. Donohoe¹⁸,

G. Robertson⁵², A.B. Rodrigues⁴³, E. Rodrigues⁵⁴, J.A. Rodriguez Lopez⁶⁸,
 E. Rodriguez Rodriguez⁴⁰, A. Rollings⁵⁷, P. Roloff⁴², V. Romanovskiy³⁸,
 M. Romero Lamas⁴⁰, A. Romero Vidal⁴⁰, J.D. Roth^{77,†}, M. Rotondo²³,
 M.S. Rudolph⁶², T. Ruf⁴², R.A. Ruiz Fernandez⁴⁰, J. Ruiz Vidal⁴¹, A. Ryzhikov³⁸,
 J. Ryzka³⁴, J.J. Saborido Silva⁴⁰, N. Sagidova³⁸, N. Sahoo⁴⁷, B. Saitta^{27,h},
 M. Salomoni⁴², C. Sanchez Gras³², R. Santacesaria³⁰, C. Santamarina Rios⁴⁰,
 M. Santimaria²³, E. Santovetti^{31,u}, D. Saranin³⁸, G. Sarpis¹⁴, M. Sarpis⁶⁹,
 A. Sarti³⁰, C. Satriano^{30,t}, A. Satta³¹, M. Saur¹⁵, D. Savrina³⁸, H. Sazak⁹,
 L.G. Scantlebury Smead⁵⁷, A. Scarabotto¹³, S. Schael¹⁴, S. Scherl⁵⁴, M. Schiller⁵³,
 H. Schindler⁴², M. Schmelling¹⁶, B. Schmidt⁴², S. Schmitt¹⁴, O. Schneider⁴³,
 A. Schopper⁴², M. Schubiger³², S. Schulte⁴³, M.H. Schune¹¹, R. Schwemmer⁴²,
 B. Sciascia^{23,42}, A. Sciuccati⁴², S. Sellam⁴⁰, A. Semennikov³⁸, M. Senghi Soares³³,
 A. Sergi^{24,k}, N. Serra⁴⁴, L. Sestini²⁸, A. Seuthe¹⁵, Y. Shang⁵, D.M. Shangase⁷⁷,
 M. Shapkin³⁸, I. Shchemerov³⁸, L. Shchutska⁴³, T. Shears⁵⁴, L. Shekhtman³⁸,
 Z. Shen⁵, S. Sheng^{4,6}, V. Shevchenko³⁸, E.B. Shields^{26,n}, Y. Shimizu¹¹,
 E. Shmanin³⁸, J.D. Shupperd⁶², B.G. Siddi^{21,i}, R. Silva Coutinho⁴⁴, G. Simi²⁸,
 S. Simone^{19,f}, N. Skidmore⁵⁶, R. Skuza¹⁷, T. Skwarnicki⁶², M.W. Slater⁴⁷,
 I. Slazyk^{21,i}, J.C. Smallwood⁵⁷, J.G. Smeaton⁴⁹, E. Smith⁴⁴, M. Smith⁵⁵,
 A. Snoch³², L. Soares Lavra⁹, M.D. Sokoloff⁵⁹, F.J.P. Soler⁵³, A. Solomin^{38,48},
 A. Solovev³⁸, I. Solovyev³⁸, F.L. Souza De Almeida², B. Souza De Paula²,
 B. Spaan^{15,†}, E. Spadaro Norella^{25,m}, E. Spiridenkov³⁸, P. Spradlin⁵³, F. Stagni⁴²,
 M. Stahl⁵⁹, S. Stahl⁴², S. Stanislaus⁵⁷, O. Steinkamp⁴⁴, O. Stenyakin³⁸,
 H. Stevens¹⁵, S. Stone^{62,†}, D. Strelakina³⁸, F. Suljik⁵⁷, J. Sun²⁷, L. Sun⁶⁷,
 Y. Sun⁶⁰, P. Svihra⁵⁶, P.N. Swallow⁴⁷, K. Swientek³⁴, A. Szabelski³⁶,
 A. Szczepaniak^{62,y}, T. Szumlak³⁴, M. Szymanski⁴², S. Taneja⁵⁶, A.R. Tanner⁴⁸,
 M.D. Tat⁵⁷, A. Terentev³⁸, F. Teubert⁴², E. Thomas⁴², D.J.D. Thompson⁴⁷,
 K.A. Thomson⁵⁴, H. Tilquin⁵⁵, V. Tisserand⁹, S. T'Jampens⁸, M. Tobin⁴,
 L. Tomassetti^{21,i}, X. Tong⁵, D. Torres Machado¹, D.Y. Tou³, E. Trifonova³⁸,
 S.M. Trilov⁴⁸, C. Trippel⁴³, G. Tuci⁶, A. Tully⁴³, N. Tuning^{32,42}, A. Ukleja^{36,42},
 D.J. Unverzagt¹⁷, E. Ursov³⁸, A. Usachov³², A. Ustyuzhanin³⁸, U. Uwer¹⁷,
 A. Vagner³⁸, V. Vagnoni²⁰, A. Valassi⁴², G. Valenti²⁰, N. Valls Canudas⁷⁵,
 M. van Beuzekom³², M. Van Dijk⁴³, H. Van Hecke⁶¹, E. van Herwijnen³⁸,
 M. van Veghel⁷³, R. Vazquez Gomez³⁹, P. Vazquez Regueiro⁴⁰, C. Vázquez Sierra⁴²,
 S. Vecchi²¹, J.J. Velthuis⁴⁸, M. Veltri^{22,w}, A. Venkateswaran⁶², M. Veronesi³²,
 M. Vesterinen⁵⁰, D. Vieira⁵⁹, M. Vieites Diaz⁴³, H. Viemann⁷⁰, X. Vilasis-Cardona⁷⁵,
 E. Vilella Figueras⁵⁴, A. Villa²⁰, P. Vincent¹³, F.C. Volle¹¹, D. vom Bruch¹⁰,
 A. Vorobyev³⁸, V. Vorobyev³⁸, N. Voropaev³⁸, K. Vos⁷⁴, R. Waldi¹⁷, J. Walsh²⁹,
 C. Wang¹⁷, J. Wang⁵, J. Wang⁴, J. Wang³, J. Wang⁶⁷, M. Wang⁵, R. Wang⁴⁸,
 Y. Wang⁷, Z. Wang⁴⁴, Z. Wang³, Z. Wang⁶, J.A. Ward^{50,63}, N.K. Watson⁴⁷,
 D. Websdale⁵⁵, C. Weisser⁵⁸, B.D.C. Westhenry⁴⁸, D.J. White⁵⁶, M. Whitehead⁴⁸,
 A.R. Wiederhold⁵⁰, D. Wiedner¹⁵, G. Wilkinson⁵⁷, M.K. Wilkinson⁶², I. Williams⁴⁹,
 M. Williams⁵⁸, M.R.J. Williams⁵², F.F. Wilson⁵¹, W. Wislicki³⁶, M. Witek³⁵,
 L. Witola¹⁷, G. Wormser¹¹, S.A. Wotton⁴⁹, H. Wu⁶², K. Wyllie⁴², Z. Xiang⁶,
 D. Xiao⁷, Y. Xie⁷, A. Xu⁵, J. Xu⁶, L. Xu³, M. Xu⁵⁰, Q. Xu⁶, Z. Xu⁹,
 Z. Xu⁶, D. Yang³, S. Yang⁶, Y. Yang⁶, Z. Yang⁵, Z. Yang⁶⁰, Y. Yao⁶²,
 L.E. Yeomans⁵⁴, H. Yin⁷, J. Yu⁶⁵, X. Yuan⁶², E. Zaffaroni⁴³, M. Zavertyaev¹⁶,
 M. Zdybal³⁵, O. Zenaiev⁴², M. Zeng³, D. Zhang⁷, L. Zhang³, S. Zhang⁶⁵,
 S. Zhang⁵, Y. Zhang⁵, Y. Zhang⁵⁷, A. Zharkova³⁸, A. Zhelezov¹⁷, Y. Zheng⁶,
 T. Zhou⁵, X. Zhou⁶, Y. Zhou⁶, V. Zhovkovska¹¹, X. Zhu³, X. Zhu⁷, Z. Zhu⁶,
 V. Zhukov^{14,38}, Q. Zou^{4,6}, S. Zucchelli^{20,g}, D. Zuliani²⁸, G. Zunica⁵⁶.

- ¹ *Centro Brasileiro de Pesquisas Físicas (CBPF), Rio de Janeiro, Brazil*
- ² *Universidade Federal do Rio de Janeiro (UFRJ), Rio de Janeiro, Brazil*
- ³ *Center for High Energy Physics, Tsinghua University, Beijing, China*
- ⁴ *Institute Of High Energy Physics (IHEP), Beijing, China*
- ⁵ *School of Physics State Key Laboratory of Nuclear Physics and Technology, Peking University, Beijing, China*
- ⁶ *University of Chinese Academy of Sciences, Beijing, China*
- ⁷ *Institute of Particle Physics, Central China Normal University, Wuhan, Hubei, China*
- ⁸ *Université Savoie Mont Blanc, CNRS, IN2P3-LAPP, Annecy, France*
- ⁹ *Université Clermont Auvergne, CNRS/IN2P3, LPC, Clermont-Ferrand, France*
- ¹⁰ *Aix Marseille Univ, CNRS/IN2P3, CPPM, Marseille, France*
- ¹¹ *Université Paris-Saclay, CNRS/IN2P3, IJCLab, Orsay, France*
- ¹² *Laboratoire Leprince-Ringuet, CNRS/IN2P3, Ecole Polytechnique, Institut Polytechnique de Paris, Palaiseau, France*
- ¹³ *LPNHE, Sorbonne Université, Paris Diderot Sorbonne Paris Cité, CNRS/IN2P3, Paris, France*
- ¹⁴ *I. Physikalisches Institut, RWTH Aachen University, Aachen, Germany*
- ¹⁵ *Fakultät Physik, Technische Universität Dortmund, Dortmund, Germany*
- ¹⁶ *Max-Planck-Institut für Kernphysik (MPIK), Heidelberg, Germany*
- ¹⁷ *Physikalisches Institut, Ruprecht-Karls-Universität Heidelberg, Heidelberg, Germany*
- ¹⁸ *School of Physics, University College Dublin, Dublin, Ireland*
- ¹⁹ *INFN Sezione di Bari, Bari, Italy*
- ²⁰ *INFN Sezione di Bologna, Bologna, Italy*
- ²¹ *INFN Sezione di Ferrara, Ferrara, Italy*
- ²² *INFN Sezione di Firenze, Firenze, Italy*
- ²³ *INFN Laboratori Nazionali di Frascati, Frascati, Italy*
- ²⁴ *INFN Sezione di Genova, Genova, Italy*
- ²⁵ *INFN Sezione di Milano, Milano, Italy*
- ²⁶ *INFN Sezione di Milano-Bicocca, Milano, Italy*
- ²⁷ *INFN Sezione di Cagliari, Monserrato, Italy*
- ²⁸ *Università degli Studi di Padova, Università e INFN, Padova, Padova, Italy*
- ²⁹ *INFN Sezione di Pisa, Pisa, Italy*
- ³⁰ *INFN Sezione di Roma La Sapienza, Roma, Italy*
- ³¹ *INFN Sezione di Roma Tor Vergata, Roma, Italy*
- ³² *Nikhef National Institute for Subatomic Physics, Amsterdam, Netherlands*
- ³³ *Nikhef National Institute for Subatomic Physics and VU University Amsterdam, Amsterdam, Netherlands*
- ³⁴ *AGH - University of Science and Technology, Faculty of Physics and Applied Computer Science, Kraków, Poland*
- ³⁵ *Henryk Niewodniczanski Institute of Nuclear Physics Polish Academy of Sciences, Kraków, Poland*
- ³⁶ *National Center for Nuclear Research (NCBJ), Warsaw, Poland*
- ³⁷ *Horia Hulubei National Institute of Physics and Nuclear Engineering, Bucharest-Magurele, Romania*
- ³⁸ *Affiliated with an institute covered by a cooperation agreement with CERN*
- ³⁹ *ICCUB, Universitat de Barcelona, Barcelona, Spain*
- ⁴⁰ *Instituto Galego de Física de Altas Enerxías (IGFAE), Universidade de Santiago de Compostela, Santiago de Compostela, Spain*
- ⁴¹ *Instituto de Física Corpuscular, Centro Mixto Universidad de Valencia - CSIC, Valencia, Spain*
- ⁴² *European Organization for Nuclear Research (CERN), Geneva, Switzerland*
- ⁴³ *Institute of Physics, Ecole Polytechnique Fédérale de Lausanne (EPFL), Lausanne, Switzerland*
- ⁴⁴ *Physik-Institut, Universität Zürich, Zürich, Switzerland*
- ⁴⁵ *NSC Kharkiv Institute of Physics and Technology (NSC KIPT), Kharkiv, Ukraine*
- ⁴⁶ *Institute for Nuclear Research of the National Academy of Sciences (KINR), Kyiv, Ukraine*
- ⁴⁷ *University of Birmingham, Birmingham, United Kingdom*
- ⁴⁸ *H.H. Wills Physics Laboratory, University of Bristol, Bristol, United Kingdom*
- ⁴⁹ *Cavendish Laboratory, University of Cambridge, Cambridge, United Kingdom*
- ⁵⁰ *Department of Physics, University of Warwick, Coventry, United Kingdom*
- ⁵¹ *STFC Rutherford Appleton Laboratory, Didcot, United Kingdom*

- ⁵² *School of Physics and Astronomy, University of Edinburgh, Edinburgh, United Kingdom*
- ⁵³ *School of Physics and Astronomy, University of Glasgow, Glasgow, United Kingdom*
- ⁵⁴ *Oliver Lodge Laboratory, University of Liverpool, Liverpool, United Kingdom*
- ⁵⁵ *Imperial College London, London, United Kingdom*
- ⁵⁶ *Department of Physics and Astronomy, University of Manchester, Manchester, United Kingdom*
- ⁵⁷ *Department of Physics, University of Oxford, Oxford, United Kingdom*
- ⁵⁸ *Massachusetts Institute of Technology, Cambridge, Massachusetts, United States*
- ⁵⁹ *University of Cincinnati, Cincinnati, Ohio, United States*
- ⁶⁰ *University of Maryland, College Park, Maryland, United States*
- ⁶¹ *Los Alamos National Laboratory (LANL), Los Alamos, New Mexico, United States*
- ⁶² *Syracuse University, Syracuse, New York, United States*
- ⁶³ *School of Physics and Astronomy, Monash University, Melbourne, Australia, associated to ⁵⁰*
- ⁶⁴ *Pontifícia Universidade Católica do Rio de Janeiro (PUC-Rio), Rio de Janeiro, Brazil, associated to ²*
- ⁶⁵ *Physics and Micro Electronic College, Hunan University, Changsha City, China, associated to ⁷*
- ⁶⁶ *Guangdong Provincial Key Laboratory of Nuclear Science, Guangdong-Hong Kong Joint Laboratory of Quantum Matter, Institute of Quantum Matter, South China Normal University, Guangzhou, China, associated to ³*
- ⁶⁷ *School of Physics and Technology, Wuhan University, Wuhan, China, associated to ³*
- ⁶⁸ *Departamento de Física, Universidad Nacional de Colombia, Bogota, Colombia, associated to ¹³*
- ⁶⁹ *Universität Bonn - Helmholtz-Institut für Strahlen und Kernphysik, Bonn, Germany, associated to ¹⁷*
- ⁷⁰ *Institut für Physik, Universität Rostock, Rostock, Germany, associated to ¹⁷*
- ⁷¹ *Eotvos Lorand University, Budapest, Hungary, associated to ⁴²*
- ⁷² *INFN Sezione di Perugia, Perugia, Italy, associated to ²¹*
- ⁷³ *Van Swinderen Institute, University of Groningen, Groningen, Netherlands, associated to ³²*
- ⁷⁴ *Universiteit Maastricht, Maastricht, Netherlands, associated to ³²*
- ⁷⁵ *DS4DS, La Salle, Universitat Ramon Llull, Barcelona, Spain, associated to ³⁹*
- ⁷⁶ *Department of Physics and Astronomy, Uppsala University, Uppsala, Sweden, associated to ⁵³*
- ⁷⁷ *University of Michigan, Ann Arbor, Michigan, United States, associated to ⁶²*
- ^a *Universidade Federal do Triângulo Mineiro (UFMT), Uberaba-MG, Brazil*
- ^b *Central South U., Changsha, China*
- ^c *Hangzhou Institute for Advanced Study, UCAS, Hangzhou, China*
- ^d *Excellence Cluster ORIGINS, Munich, Germany*
- ^e *Universidad Nacional Autónoma de Honduras, Tegucigalpa, Honduras*
- ^f *Università di Bari, Bari, Italy*
- ^g *Università di Bologna, Bologna, Italy*
- ^h *Università di Cagliari, Cagliari, Italy*
- ⁱ *Università di Ferrara, Ferrara, Italy*
- ^j *Università di Firenze, Firenze, Italy*
- ^k *Università di Genova, Genova, Italy*
- ^l *Dipartimento MIFT, Università degli Studi di Messina and INFN Sezione di Catania, Italy, Messina and Catania, Italy*
- ^m *Università degli Studi di Milano, Milano, Italy*
- ⁿ *Università di Milano Bicocca, Milano, Italy*
- ^p *Università di Padova, Padova, Italy*
- ^q *Università di Perugia, Perugia, Italy*
- ^r *Scuola Normale Superiore, Pisa, Italy*
- ^s *Università di Pisa, Pisa, Italy*
- ^t *Università della Basilicata, Potenza, Italy*
- ^u *Università di Roma Tor Vergata, Roma, Italy*
- ^v *Università di Siena, Siena, Italy*
- ^w *Università di Urbino, Urbino, Italy*
- ^x *Departamento de Física Interdisciplinar, Universidad Nacional de Educación a Distancia (UNED), Madrid, Spain*
- ^y *Department of Physics, Indiana University, Bloomington, United States*
- [†] *Deceased*